# Magnetic Moments due to Rotation in Li⁶F and Li⁷F†‡

ALLAN M. RUSSELL*

*Syracuse University, Syracuse, New York*

(Received April 22, 1958)

A molecular beam electric resonance spectrometer has been used to measure the Zeeman splitting of the hyperfine structure of Li⁶F and Li⁷F in the $J=1$ rotational state. From these measurements the magnitudes of the rotational magnetic moments of these molecules were determined:

$$(\mu_J/J)_{\text{Li}^6\text{F}} = (0.0818_{-0.0003}^{+0.0005}) \text{ nuclear magnetons per } J.$$
$$(\mu_J/J)_{\text{Li}^7\text{F}} = (0.0642_{-0.0002}^{+0.0004}) \text{ nuclear magnetons per } J.$$

Since the signs of the rotational magnetic moments could not be measured, the sign of the electric dipole moment was not determined experimentally.

A complete expression for the rotational magnetic moment in a diatomic molecule is derived. When the rotational perturbation of the electron motion is neglected the complete expression is shown to reduce to an equation for the magnetic moment of two singly charged ions. This ion-pair approximation, applied to the molecule above, indicates that the values for the moments should be positive.

The nonslip electronic contribution, neglected in the ion-pair approximation, is described in terms of a semiclassical model. Numerical evaluation of the nonslip electronic contribution to the rotational magnetic moment of Li⁶F and the nuclear $J$-dependent magnetic field of the fluorine spin-rotation interaction yields results within 10% of experimental values. The model shows that these two molecular constants, though the results of the same perturbation, arise from different parts of the charge distribution.

## EXPERIMENT

**M**AGNETIC moments due to rotation have been measured in a number of $^1\Sigma$ molecules.[1] Of these, only $H_2$ is diatomic and it is covalently bonded. This report describes the first measurements made in ionically bonded diatomic $^1\Sigma$ molecules.

The measurements were made by observing the Zeeman effect in the hyperfine structure of Li⁶F and Li⁷F. The results of these measurements have been reported previously.[2]

One reason for choosing the lithium fluorides is that the fluorine spin-rotation interactions, which are closely related to the molecular magnetic moment, have been measured in both these molecules.[3,4]

## Apparatus

The measurements of the rotational magnetic moments of Li⁶F and Li⁷F were made on a molecular beam electric resonance (MOBER) spectrometer. This apparatus, designed to operate in the radio-frequency region, has been described by many authors. The most recent article[5] will serve as a description of the apparatus used in these experiments except for a few changes of which the significant one will be described below.

All experiments done previously with this apparatus made use of the Stark effect in studying the hyperfine structure of the alkali halide molecules. This is the first experiment to use the Zeeman effect. For this experiment the electric C-field was replaced by a magnetic C-field. The transitions, however, were still induced electrically.

The magnetic C-field was designed to furnish both a constant magnetic field and a constant electric field so that combined Stark-Zeeman effects could be observed. For this reason, special emphasis was placed on the requirements for a uniform electric field at the expense of uniformity in the magnetic field. This was done because the electric interaction was much larger than the magnetic and would, therefore, have a much greater effect on line width. Unfortunately the line widths in the combined case were considerably larger than theoretical calculations had predicted and were too large to permit useful data to be taken. The data used in the magnetic moment measurements were all taken at zero electric field.

Because of the limitations of space the magnetic field in the transition region was obtained through the use of a permanent magnet. An Alnico V magnet, designed to fit the space available, was cast by the Indiana Steel Products Company of Valparaiso, Indiana. It was designed to give a field strength of 10 000 gauss in a $\frac{1}{8}$-inch gap between soft-iron pole pieces. Since hardened steel was used to help keep the pole pieces flat the magnetic field was less uniform than it would have been otherwise and was about 5000 gauss.

Figure 1 is a drawing of the C-field magnet. The two poles are held together by bronze springs while held apart at the corners by four sets of opposing screws. These screws all had right-hand threads but different pitches, one side 46 threads/inch, the other 48 threads/inch. This permitted a change in the pole separation of

[1] C. H. Townes and A. L. Schawlow, *Microwave Spectroscopy* (McGraw-Hill Book Company, Inc., New York, 1955), p. 294.

[2] A. M. Russell, Phys. Rev. **106**, 1100 (1957).

[3] J. C. Swartz and J. W. Trischka, Phys. Rev. **88**, 1085 (1952).

[4] R. Braunstein and J. W. Trischka, Phys. Rev. **98**, 1092 (1955).

[5] D. T. F. Marple and J. W. Trischka, Phys. Rev. **103**, 597 (1956).

TABLE I. Mean values of $H_c$ on three different dates.

| Measurement | $t$ (days) | Field strength (gauss) |
|:---:|:---:|:---:|
| (1) | 0 | 5148±25 |
| (2) | 317 | 4815±15 |
| (3) | 363 | 4792±15 |

about 0.000050 inch when the screws were turned ten degrees together.

One pole is divided and insulated from the rest of the magnet so that both constant voltage and rf could be applied. The pole faces themselves were heavily chromium plated and slip ground. They were found to be flat to within 0.000050 inch when measured on a Sheffield visual gauge. A sapphire ball of diameter 0.1250±0.0001 inch and sphericity 0.000025 inch was used as a gauge to gap the poles.

The $C$-field magnet gap was too small to admit any ordinary proton resonance probe. For this reason the magnetic field in the gap was measured indirectly, an electromagnet serving as a reference field. The procedure was as follows:

(a) The emf in a germanium Hall probe was balanced out with a potentiometer when the probe was in the $C$-field magnet.

(b) The reference magnet was adjusted to maintain balance with the probe in the reference magnet.

(c) The magnetic field strength of the reference magnet was then determined from the proton resonance frequency.

Steps (a) and (b) were repeated until the galvanometer balanced to within 5 millimeters (about 2 gauss) before the resonance frequency was measured.

Measurements made on three different dates showed that the long-time stability of the magnet was not good and that the magnet lost field strength with time. This introduced a systematic error into the value of the magnetic field at the time the spectra were measured.

The mean values of $H_c$ for the three sets of measurements are given in Table I. The errors here are due primarily to the variation in field strength along the magnet. Since the large drift was not anticipated, it was originally intended that measurement (1) would serve as an upper bound and that measurement (2) would differ only slightly from (1), thus defining a narrow region containing the required value of magnetic field strength. Measurement (2), made shortly after the spectra were taken, indicated a large drift, however, which required that a third measurement be made to determine the latest drift rate. The last two measurements yielded a drift rate of 23 gauss in 46 days. By interpolation this yielded a value of $H_c = 4827$ gauss at the time the spectra were taken.

The ±15 gauss error still applies. The drift from (1) to (2) could, however, possibly be accounted for in the
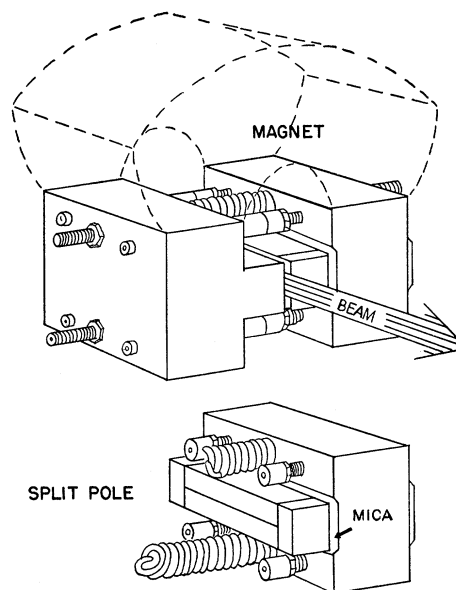


FIG. 1. The $C$-field magnet with pole pieces.

shorting of the magnet which was necessary during the exploratory stages of the experiment. The 12 gauss added to measurement (2) should therefore be included as a systematic error.

The final value of the magnetic field strength is

$$H_c = 4827_{-27}^{+15} \text{ gauss.}$$

## Predicted Spectra

The MOBER spectrometer has already been used to study the hyperfine structure of Li⁶F and Li⁷F using the Stark effect.[3,4] Each of these publications gives a detailed description of the Hamiltonian used and the predicted spectra. The only new feature introduced by the use of the magnetic filed is the removal of the degeneracy in the sign of $m_J$. The spectra which result represent a splitting of each zero field (electric) line into two parts, the splitting being the same for all lines and depending upon the magnitude of the rotational magnetic moment and the magnetic field strength.

The interaction of the nuclear spins with the external magnetic field will not affect the difference between energy levels because $m_I$ remains unchanged in the transitions studied.

Both molecules were studied in the transitions

$$(J, m_J): (1, +1) \rightarrow (1,0) \quad \text{and} \quad (1, -1) \rightarrow (1,0).$$

The selection rules are

$$\Delta m_J = \pm 1, \quad \Delta m_{I1} = 0, \quad \Delta m_{I2} = 0.$$

The interaction constants used to calculate the spectra are those given in the references cited above.

Figures 2 and 3 show the line positions to be expected for each molecule when the levels are split by the interaction of the rotational magnetic moment with the
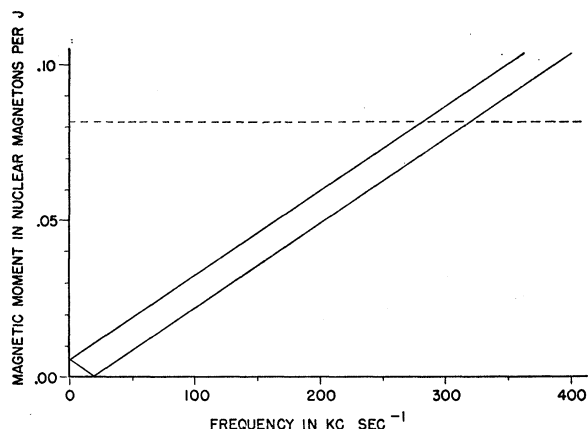
FIG. 2. Predicted line frequencies for Li$^6$F as a function of $\mu_J$ for a magnetic field of 4827 gauss.

external magnetic field. The splitting will be

$$2(\mu_J/J)m_J H,$$

or, for $J=1$,

$$2\mu_J H.$$

Thus, for a given value of magnetic field the spectra are predicted for a range of values of $\mu_J$. For purposes of indentification, the Li$^7$F lines are numbered $\nu_1 \cdots \nu_8$ in order, from the lowest frequency to the highest under the condition $\mu_J=0$. For the condition $\mu_J \neq 0$ the low-frequency components will be denoted by primes and the high-frequency by double primes. Table II gives the interaction constants used and the predicted line frequencies for each molecule under the condition $\mu_J=0$.

The reflection of the line positions at zero frequency arises because the spectrometer does not distinguish between emission and absorption lines. The predicted frequencies are, therefore, the absolute value of the energy level differences.
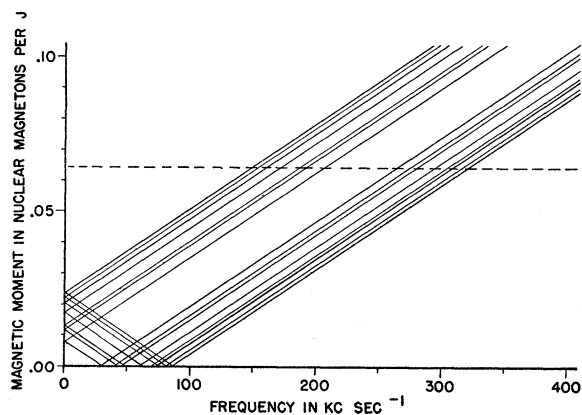


FIG. 3. Predicted line frequencies for Li$^7$F as a function of $\mu_J$ for a magnetic field of 4827 gauss.

## Results

Figure 4 shows the observed lines for Li$^6$F. Their frequencies are

$$\nu' = 282.0 \pm 0.2 \text{ kc sec}^{-1},$$

$$\nu'' = 319.5 \pm 0.2 \text{ kc sec}^{-1}.$$

From the predicted spectra (Fig. 2) it is clear that

$$\gamma = \tfrac{1}{2}(\nu' + \nu'') = 300.8 \pm 0.2 \text{ kc sec}^{-1},$$

where

$$\mu_J(J=1) = \frac{\mu_J}{J} = \frac{1}{\mu_n} \frac{h\nu}{H_c} = 1.312 \times 10^{-3} \frac{\gamma}{H_c}.$$

Substitution of the value for Li$^6$F and the value for $H_c$ yields,

$$\left( \frac{\mu_J}{J} \right)_{\text{Li}^6\text{F}} = 0.0818_{-0.0003}^{+0.0005} \text{ nm}/J.$$

TABLE II. Molecular constants and predicted line frequencies assuming $\mu_J=0$ for the $(J, m_J)$: $(1, \pm 1) \rightarrow (1,0)$ transitions in Li$^6$F and Li$^7$F.

| Li$^6$F | | |
|---|---|---|
| $eqQ_1/h=0$ | | $eqQ_2/h=0$ |
| $c_1/h=0$ | | $c_2/h=+36.8$ kc sec$^{-1}$ |
| | $g_1 g_2 \mu_N^2 / r^3 h \cong 0$ | |
| | $\nu = 18.4$ kc sec$^{-1}$ | |

| Li$^7$F | | |
|---|---|---|
| $eqQ_1/h=+412$ kc sec$^{-1}$ | | $eqQ_2/h=0$ |
| $c_1/h=+$ kc sec$^{-1}$ | | $c_2/h=+33$ kc sec$^{-1}$ |
| | $g_1 g_2 \mu_N^2 / r^2 h = +12$ kc sec$^{-1}$ | |
| $\nu_1 = 30.3$ kc sec$^{-1}$ | | $\nu_5 = 69.9$ kc sec$^{-1}$ |
| $\nu_2 = 42.5$ kc sec$^{-1}$ | | $\nu_6 = 73.3$ kc sec$^{-1}$ |
| $\nu_3 = 48.1$ kc sec$^{-1}$ | | $\nu_7 = 83.3$ kc sec$^{-1}$ |
| $\nu_4 = 60.3$ kc sec$^{-1}$ | | $\nu_8 = 86.7$ kc sec$^{-1}$ |

The observed spectra for Li$^7$F were much more difficult to analyze. Not only are there more lines but some predicted lines fail to appear and some spectra were observed that could only be explained in terms of double quantum transitions.

Figure 5 shows the observed spectra for Li$^7$F. Scanning up to 1600 kc sec$^{-1}$ yielded no more lines so that it can safely be assumed that no spectra lie outside the region shown. It is clear that, with a natural line width of 20 kc sec$^{-1}$ expected from the apparatus, resolution of the predicted lines could not be expected. The assignment was based, therefore, upon the gross features of the observed structure. Fortunately the two sets of lines resulting from the Zeeman splitting should be separated by twice $\nu_1$ or 60.6 kc sec$^{-1}$ (see Fig. 3). This gap is much larger than the individual separation within each set and serves as a preliminary identification of the splitting due to the magnetic field.

The final Zeeman splitting is based upon the assignment of $\nu_2'$, $\nu_1'$ and $\nu_1''$, $\nu_2''$ to the two lines on either side of the gap as shown in Fig. 6. The separation of

these two observed lines is 72.5 kc sec⁻¹. This is just twice the average of $\nu_1$ and $\nu_2$ predicted for the case (see Fig. 3 and Table II). The center of the gap may now be taken as the frequency shift, therefore,

$$\gamma = \frac{1}{2}\left(\frac{\nu_2{}'+\nu_1{}'}{2} + \frac{\nu_1{}''+\nu_2{}''}{2}\right) = 236.2 \pm 0.2 \text{ kc sec}^{-1}.$$

These frequencies were determined by the point-by-point plot of the lines as was done for Li⁶F. This plot is shown in Fig. 6.

The final value for the rotational magnetic moment for Li⁷F is

$$\left(\frac{\mu_J}{J}\right)_{\text{Li}^7\text{F}} = 0.0642_{-0.0002}{}^{+0.0004} \text{ nm}/J.$$

It should be noted that the error associated with the measured values of the moments are due to the error
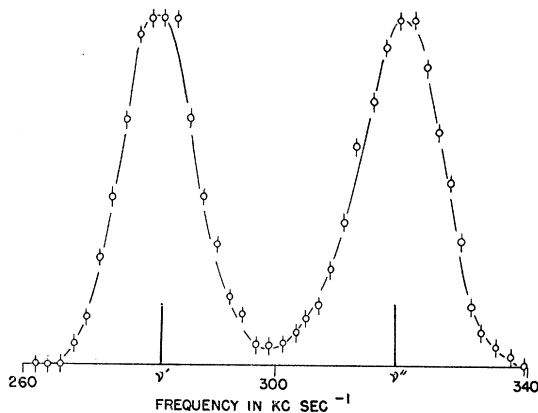


FIG. 4. Observed spectra for Li⁶F.

in the determination of the magnetic field. The errors involved in the determination of the line frequencies are much smaller and do not contribute significantly to the final error.

### SEMICLASSICAL MODEL FOR ROTATIONAL MAGNETIC MOMENTS IN ALKALI HALIDE MOLECULES

In nonrotating ¹Σ molecules the orbital angular momentum of the nuclei about the center of mass and the total orbital angular momentum of the electrons about the center of mass are both zero. There is, therefore, no magnetic dipole moment associated with the molecule if nuclear moments are neglected. When such a molecule is rotating, however, neither the nuclear nor the electronic angular momentum about the center of mass is zero. In this case a molecular magnetic dipole moment $\mu_J$ may exist, its magnitude varying directly with rotational state.

The model which will be described applies to rotational magnetic moments which arise in ionic diatomic
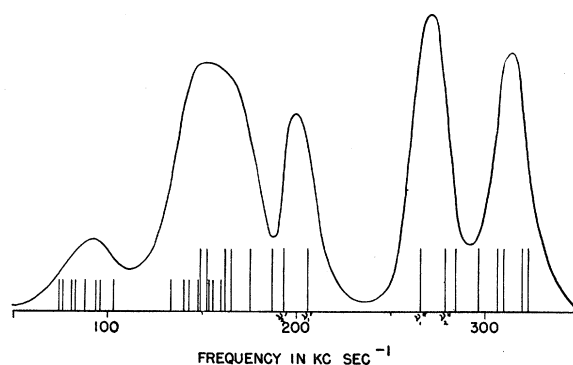


FIG. 5. Recorded Li⁷F spectra redrawn so as to be rectilinear.

molecules, in particular, the alkali halides. These molecules have ¹Σ ground states, permanent electric dipole moments and are subject to certain simplifying approximations which will be discussed farther on. For these molecules the magnitude of the rotational magnetic moment referred to the $J=1$ rotational state depends upon three terms:

(A) The nuclear term arising from the angular momentum of the positively charged nuclei about the center of mass of the molecule.

(B) The main electronic contribution which stems from the angular momentum of the electrons about the center of mass when it is explicitly assumed that the motion of electrons about parent nuclei is undisturbed by the rotation of the molecule. Electrons which behave in this way are sometimes called "slipping electrons".

(C) The nonslip electronic contribution. This term is a correction on (B) due to the perturbation of the electronic motion by the rotation of the molecule.

To clarify the discussion of the rotational magnetic moment, the following notation will be adopted with the subscripts denoting the terms as described above:
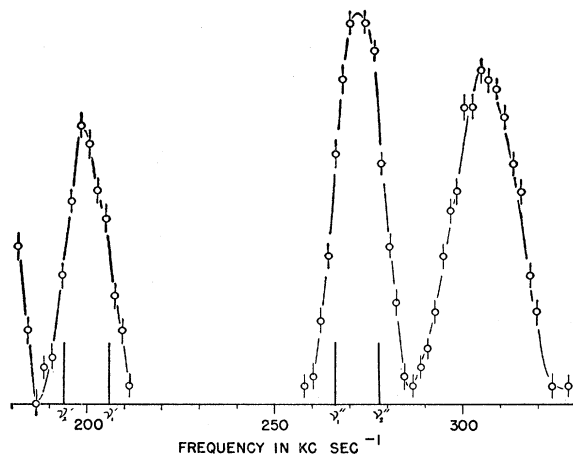
$$\mu_{ABC} \equiv \mu_A + \mu_B + \mu_C \equiv \mu_J.$$



FIG. 6. Observed spectra for Li⁷F.

In rotating diatomic molecules which have no permanent electric dipole moment, terms $A$ and $B$ are equal and opposite. The total rotational magnetic moment is, therefore, represented by the term $C$.[6] In the alkali halides, however, the terms $A$ and $B$ are not equal in magnitude so that there is a net contribution for which term $C$ may be considered a correction.

In this section a theoretical expression for $\mu_{ABC}$ will be derived for the case of an ionic diatomic molecule. This expression will be the form $(\mu_A + \mu_{BC})$. Unfortunately this is not convenient since several estimates exist for $\mu_C$ alone. By making the ion-pair approximation it will be possible to reduce the complete expression for $\mu_{ABC}$ to a simple classical expression for $\mu_{AB}$. A semiclassical model for $\mu_C$, the nonslip electronic contribution, will then be described.

This nonslip electronic contribution is of particular interest because of its relation to the spin-rotation interaction of a nuclear spin with the magnetic field created at the nucleus due to a perturbation of the electronic motion. This is the same perturbation which gives rise to $C$.

## Complete Solution, $\mu_{ABC}$

The solution described below follows the analysis of Eshbach and Strandberg[7] but is limited to diatomic molecules. It will later be specialized to include only ionic diatomic molecules. The solution, while called complete, is nevertheless not exact and the following approximations are made. The molecule is considered rigid so that rotational stretching and vibrational effects are not included. In addition, it is assumed that the molecular motion is not perturbed by the electronic motion.

The Hamiltonian for the system neglecting rotational stretching, vibration, and omitting the translational term is,

$$\mathcal{3C} = \tfrac{1}{2}L^2/I + \tfrac{1}{2}m\sum_j p_j{}^2 + V, \tag{1}$$

where $L$ is the angular momentum of the nuclei, $p_j$ is the linear momentum of the $j$th electron, and $I$ is the total moment of inertia. The total angular momentum is a constant of the motion and is given by

$$\mathcal{L} = \mathbf{L} + \mathbf{l},$$

where $\mathbf{l}$ is the total electronic angular momentum. Therefore, since

$$L^2 = \mathbf{L}\cdot\mathbf{L} = (\mathcal{L}-\mathbf{l})\cdot(\mathcal{L}-\mathbf{l}) = \mathcal{L}^2 - 2\mathcal{L}l + l^2,$$

the Hamiltonian may be written

$$\mathcal{3C} = \tfrac{1}{2}\mathcal{L}^2/I - \mathcal{L}l/I + \tfrac{1}{2}l^2/I + \tfrac{1}{2}m\sum_j p_j{}^2 + V. \tag{2}$$

Since the angular momentum of the electrons in $^1\!\sum$ molecules is much smaller than the total angular momentum, the third term in equation (2) is omitted and the second term is considered as a perturbation on the electronic motion. The final expression may be separated into a nuclear Hamiltonian and an electronic Hamiltonian with a perturbation term,

$$\mathcal{3C}_n = \tfrac{1}{2}\mathcal{L}^2/I, \quad \mathcal{3C}_e = \mathcal{3C}_e{}^0 + \mathcal{3C}_e{}^1,$$

where $\mathcal{3C}_e{}^0 = \tfrac{1}{2}m\sum_j p_j{}^2 + V$ and $\mathcal{3C}_e{}^1 = -\mathcal{L}l/I$.

The nuclear contribution to the rotational magnetic moment may be written[8]

$$\mu_A = -\frac{e\omega}{2c}(Z_+R_+{}^2 + Z_-R_-{}^2). \tag{3}$$

The electronic contribution may be written in terms of the expectation value for the angular momentum in the $J$ direction, where $\mathbf{l}$ depends upon $\mathbf{L}$ through $\mathcal{3C}_e{}^1$.

$$\mu_{BC} = (e/2mc)l_Z. \tag{4}$$

The first order wave function may then be written

$$\psi_0{}' = \psi_0{}^0 + \sum_n{}' \frac{\mathcal{L}_Z}{I}\left[\frac{(n|l_Z|0)}{E_n - E_0}\right]\psi_n{}^0.$$

To first order, then, the expectation value for $l_Z$ is

$$(0|l_Z|0)' = (0|l_Z|0) + \sum_n{}' 2\mathcal{L}_Z/I\frac{|(0|l_Z|n)|^2}{E_n - E_0}.$$

The substitution of this expression into (4) yields

$$\mu_{BC} = (e\mathcal{L}_Z/mcI)\sum_n{}'|(0|l_Z|n)|^2/(E_n - E_0),$$

but $\mathcal{L}_Z = J\hbar$ and the classical frequency corresponding to this may be defined as $\omega = J\hbar/I$, and therefore

$$\mu_{BC} = \frac{e\omega}{mc}\sum_n \frac{|(0|l_Z|n)|^2}{E_n - E_0}. \tag{5}$$

This represents the electronic contribution and is equivalent to the expression derived by Wick.[9]

The total rotational magnetic moment for diatomic molecules may now be written

$$\mu_{ABC} = -\frac{e\omega}{2c}\left[(Z_+R_+{}^2 + Z_-R_-{}^2) - \frac{2}{m}\sum_n \frac{|(0|l_Z|n)|^2}{E_n - E_0}\right]. \tag{6}$$

## Ion-Pair Approximation, $\mu_{AB}$

Eshbach and Strandberg,[7] Ramsey,[10] Townes,[1] and others have developed theoretical expressions for the rotational magnetic moment which can be applied to diatomic molecules. These expressions are exceedingly cumbersome, however, and the very great difficulties associated with obtaining electronic wave functions for

---

[6] This term is usually negative since it corresponds to the rotation of negative charges. The main exception to this is hydrogen.
[7] J. R. Eshbach and M. W. P. Stranberg, Phys. Rev. **85**, 24 (1951).

[8] See Appendix.
[9] G. C. Wick, Phys. Rev. **83**, 51 (1948).
[10] N. F. Ramsey, Phys. Rev. **87**, 1075 (1952).

a molecule prohibit the evaluation of these expressions except in the case of very simple molecules such as H$_2$. Wick,[9] Foley,[11] and White[12] develop expressions for $\mu_C$, the nonslip electronic contribution which will be described later. Foley and White give values which can be used to predict this contribution.

While a neutral atom approach must lead to the correct result in an exact theory, it does not, for alkali halides, represent the best approximation. Much success in predicting molecular constants has been achieved by considering these molecules to be composed of two ions.[13,14] This approximation is the one which will be used in the theory described below.

If the molecule is assumed to be composed of two ions whose electrons are under the influence of spherically symmetric fields only, Eq. (6) can be reduced as follows. The angular momentum of a spherical shell of electrons around a nucleus which is a distance $R$ from the center of mass is

$$l_n = l_z + Rp',$$

where $l_z$ is the angular momentum around the center of mass and $p'$ is the linear momentum of the shell in the $y$ direction. For $^1\Sigma$ molecules, however, $(0|l_n|n)=0$; therefore,

$$\sum_n' \frac{|(0|l_z|n)|^2}{E_n - E_0} = R^2 \sum_n' \frac{|(0|p'|n)|^2}{E_n - E_0},$$

and since[15]

$$\sum_n' \frac{|(0|p'|n)|^2}{E_n - E_0} = -\frac{m}{2},$$

the electronic contribution may be written

$$\sum_n' \frac{|(0|l_z|n)|^2}{E_n - E_0} = -\tfrac{1}{2}R^2 m.$$

If $Z'$ are the number of electrons associated with the nucleus of atomic number $Z$, then from (6),

$$\mu_{AB} = -\frac{e\omega}{2c}[Z_+ R_+^2 + Z_- R_-^2 - (Z_+' R_+^2 + Z_-' R_-^2)].$$

For the alkali halides, however,

$$Z_+ - Z_+' = 1 \quad \text{and} \quad Z_- - Z_-' = -1,$$

therefore,

$$\mu_{AB} = -\frac{e\omega}{2c}(R_+^2 - R_-^2).$$

[11] H. M. Foley, Phys. Rev. **72**, 504 (1947).
[12] R. L. White, Revs. Modern Phys. **27**, 276 (1955).
[13] E. S. Rittner, J. Chem. Phys. **19**, 865 (1951).
[14] G. C. Benson and B. M. E. van der Hoff, J. Chem. Phys. **22**, 469 (1954).
[15] Reference 1, p. 213.

From this follows the ion-pair result (see Appendix)

$$\frac{\mu_{AB}}{J} \cong \frac{1}{m_+} - \frac{1}{m_-}.$$

The assumption that the molecule is strictly in a $^1\Sigma$ state even though rotating is equivalent to saying that the electronic motion is unperturbed by the molecular rotation and, therefore, that $\mu_C = 0$.

In order to achieve an understanding of the origin of the nonslip electronic contribution $\mu_C$, a semiclassical model will be constructed that will also illustrate the relationship between this electronic term and the magnetic field at the fluorine nucleus. The latter gives rise to the spin-rotation interaction.

## Electronic Contribution, $\mu_C$

The model described below is intended to show the origin of the nonslip electronic contributions (I) to the molecular magnetic moment due to rotation and (II) to the magnetic field at a nucleus which gives rise to the spin-rotation or $\mathbf{I} \cdot \mathbf{J}$ interaction. It applies to ionically bonded diatomic molecules such as the alkali halides. Electrons are associated with one or the other of the nuclei in such cases and not with the molecule as a whole.

If one considers the charge cloud associated with the position probability density of the electrons, the electrons lose their individual identity in the average motion of this charge cloud. Because the electrostatic field near a nucleus is nearly spherically symmetric and because of shielding by electrons which are farther from a nucleus, electronic charge finding itself near a nucleus will be instantaneously less affected by the molecular rotation than electronic charge at a greater distance from the nucleus. Under these circumstances, electronic charge associated with $p$ or $s$ electrons will slip when it is near a nucleus and will rotate with the molecule when it is far from a nucleus. One has a picture, then, of spherical "shells" of electronic charge density rotating around a nucleus with different rotational frequencies, or more exactly, of a viscous fluid whose angular frequency, very small near the nucleus, increases uniformly to an upper limit at a point far from the nucleus. This upper limit would be the rotational frequency of the molecular frame.

The rotation of the charge cloud will be described by $\omega(r)$, where $\omega(r) = \alpha(r)\omega_J$. The symbol $\omega_J$ represents the classical angular velocity of the molecule in the rotational state $J$ and $\alpha(r)$ is the slip function which should satisfy the conditions:

$$\alpha(0) = 0, \qquad \left(\frac{d\alpha}{dr}\right)_{r=0} = 0,$$

$$\alpha(r_{\max}) \cong 1, \qquad \left(\frac{d\alpha}{dr}\right)_{r=r_{\max}} \cong 0,$$
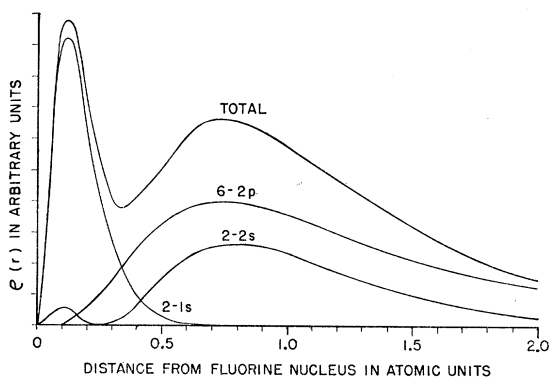
FIG. 7. Electronic charge distribution for F⁻ (from Brown[16]).

where $r_{max}$ is the value of $r$ for which $\rho(r) \cong 0$. $\alpha(r)$ is a measure of the departure of the electrostatic field from spherical symmetry at a distance $r$ from the reference nucleus.

The magnetic field at a nucleus due to charge motion such as that described above may be written,

$$H_n = \frac{2}{3} \frac{\omega_J}{c} \int_0^\infty \frac{1}{r} \alpha(r)\rho(r)dr, \qquad (7)$$

where $\rho(r)$ is the charge between $r$ and $r+dr$ in esu.

The general expression for the rotational magnetic moment due to the motion of charged particles may be expressed in terms of the angular momentum of the charged particles,

$$\mathbf{\mu} = (e/2mc)\mathbf{l}. \qquad (8)$$

The first step in determining $\mu_{BC}$ is to calculate the angular momentum of a spherical shell which rotates about a nucleus with angular velocity $\omega$ while the nucleus rotates about the center of mass of the molecule with angular velocity $\omega_J$. The angular momentum is to be calculated with respect to the center of mass of the molecule.

The angular momentum about the nucleus is

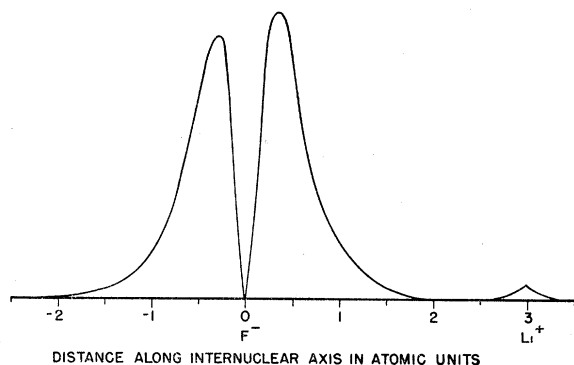$$l_N = \tfrac{2}{3}mr^2\omega, \qquad (9)$$



DISTANCE ALONG INTERNUCLEAR AXIS IN ATOMIC UNITS

FIG. 8. The $2p$ electronic charge distribution for LiF (from Benson and van der Hoff[14]).

where $m$ is the mass of the shell and $r$ is the radius. The angular momentum of the center of mass of the charged shell about the center of mass of the molecule is

$$l_{c.m.} = mR^2\omega_J, \qquad (10)$$

where $R$ is the diatance from the nucleus to the center of mass of the molecule. The total angular momentum is the sum of (9) and (10), or

$$l = \tfrac{2}{3}mr^2\omega + mR^2\omega_J. \qquad (11)$$

The substitution of (11) into (8) and the expression of $\omega$ in terms of $\alpha(r)\omega_J$ and the charge distribution in terms of $\rho(r)$ yields

$$\mu_{BC} = \frac{Z'e}{2c}R^2\omega_J - \frac{\omega_J}{3c}\int_0^\infty r^2\rho(r)\alpha(r)dr. \qquad (12)$$

Equation (12) corresponds to the total electronic contribution of one ion to the rotational magnetic moment. The first term corresponds to the contribution $\mu_B$ from completely slipping electronic charge. This term must be corrected by the second, $\mu_C$, when some of the molecular rotation is transferred to the charge cloud. The total electronic contribution from the electrons of both ions may be written

$$\mu_{BC} = \frac{e\omega_J}{2c}(Z_+'R_+{}^2 + Z_-'R_-{}^2)$$
$$- \frac{\omega_J}{3c}\left[\int_+ r^2\rho(r)\alpha(r)dr + \int_- r^2\rho(r)\alpha(r)dr\right], \qquad (13)$$

where + and − and the functions under the integral signs refer to the positive and negative ions, respectively.

The addition of the nuclear contribution to $\mu_{BC}$ yields an expression identical to the ion-pair model except for the nonslip electronic contribution. Therefore, the difference between the rotational magnetic moment as predicted by the ion-pair model, $\mu_{AB}$, and the actual experimental value should correspond to $\mu_C$, the nonslip integrals in (13).

A calculation of $H_n$ and $\mu_C$ depends upon a knowledge of the charge distribution $\rho(r)$ and the slip function $\alpha(r)$. Although neither of these functions is known, an approximate $\rho(r)$ will be constructed for Li⁶F and a guess of $\alpha(r)$ will be attempted. This will be sufficient for an illustration of the calculation. It is hoped that an $\alpha(r)$ can be found which will yield values for both $H_n$ and $\mu_C$ which will be in reasonably good agreement with the experimental values. Since two values are being fitted with one parameter there is still some measure of constraint on the model. This point will be discussed more fully later.

Efforts have been made to calculate a quantum-mechanical charge distribution for both the fluorine negative ion and the lithium fluoride molecule. In

particular, Brown[16] has calculated the charge distribution for the fluorine negative ion using Hartree-type wave functions. Figure 7 shows the results of Brown's calculations for the two $1s$, the two $2s$, and the six $2p$ electrons in F⁻.

Benson and van der Hoff[14] have determined a set of $p$ electron wave functions for the lithium fluoride molecule which are adjusted to give the proper values for the electric dipole moment and the ionization energy. From these wave functions they calculated the charge distribution shown in Fig. 8.

In order to approximate the total electronic charge distribution for the fluorine negative ion in lithium fluoride, the following adjustments were made in the distributions cited above. Since the angular features of the charge distribution are not important to the calculations, the asymmetry in Fig. 8 was averaged out by
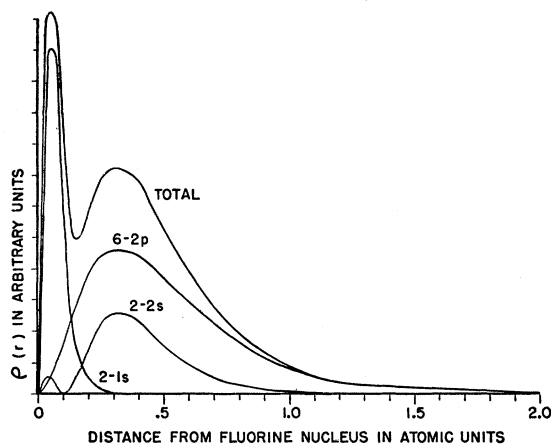


FIG. 9. Electronic charge distribution for F⁻ in LiF.

calculating $\bar{\rho}(r)$, where

$$\bar{\rho}(r) = \tfrac{1}{2}[\rho(r) + \rho(-r)],$$

The radius axis in Fig. 7 was compressed uniformly so that the second maximum in the $2s$ charge distribution occurred at the same radius as the maximum in the averaged $2p$ distribution of Fig. 8.[17] The $1s$ and $2s$ charge distributions were then each normalized to 2 and added to the $2p$ distribution for the molecule which had been normalized to 6. The result is shown in Fig. 9 and will be taken as the charge distribution about the fluorine ion in LiF.

One function which satisfies the requirements for the slip function at the extremes is the expression for the fraction of the total charge included by a sphere of radius $r$. This function was found to increase too fast near the nucleus so the slip function was chosen to be the square of the function representing the fractional
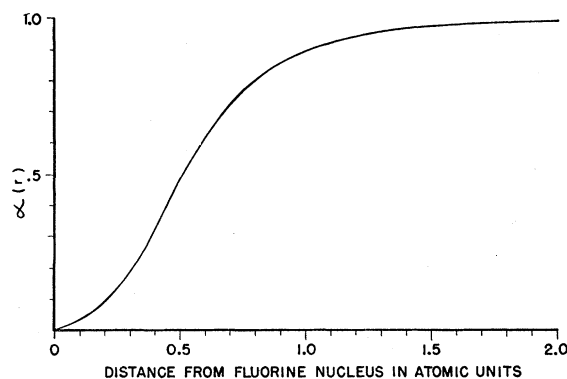


FIG. 10. The slip function.

charge, thus

$$\alpha(r) = \left[ \int_0^r \rho(r')dr' \bigg/ \int_0^\infty \rho(r')dr' \right]^2. \tag{14}$$

The slip function is shown in Fig. 10.

A numerical calculation of $H_n$ and $\mu_C$ for the model with the approximate charge distributions and the slip function described but neglecting the Li $1s$ electrons yielded the following values:

$$H_n = 8.34, \quad \mu_C = -0.033.$$

Figure 11 shows the relative contribution made by different parts of the charge distribution to the two quantities calculated. The latter two curves are normalized to the same value for the purpose of comparison. The comparison of the calculated and experimental values will be made later. The main point to be considered here is that while $H_n$ and $\mu_C$ both arise from the same perturbation, Fig. 10 shows that they stem largely from different parts of the charge distribution.

Figure 10 also shows that the contribution to $\mu_C$ from the two $1s$ electrons of the lithium ion may be
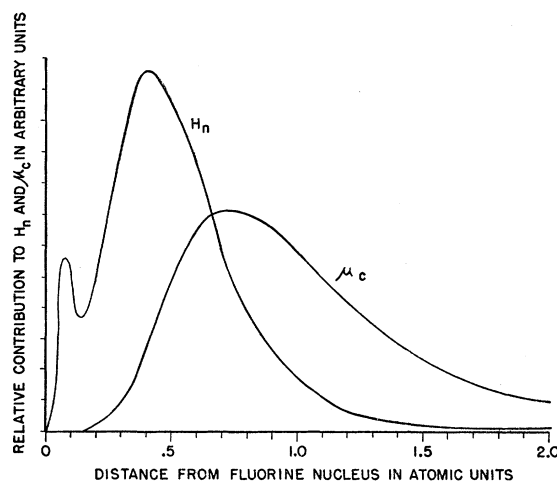


FIG. 11. Relative contributions to $H_n$ and $\mu_C$ from different parts of the charge distribution.

[16] F. W. Brown, Phys. Rev. **44**, 214 (1933).
[17] This is motivated by a desire to have the maximum in the $2s$ distribution occur at the same "orbit" as the maximum in the $2p$.

TABLE III. Comparison of measured values of the rotational magnetic moments of Li⁶F and Li⁷F (in nuclear magnetons per rotational state) with various predicted values. $\mu_{AB}$ represents the contribution of the nuclei and completely slipping electrons, $\mu_C$ is the nonslip electronic contribution, and $\mu_{ABC}$ is the total moment.

| | $\mu_{AB}$ (ion-pair) | $\mu_C$ | $\mu_{ABC}$ | |
|---|---|---|---|---|
| | +0.114 | −0.026 | +0.088 | Foley |
| Li⁶F | +0.114 | −0.040 | +0.074 | White |
| | +0.114 | −0.033 | +0.081 | Model |
| | | | $0.0818_{-0.0003}{}^{+0.0005}$ | Experimental |
| | 0.090 | −0.023 | +0.067 | Foley |
| Li⁷F | +0.090 | −0.036 | +0.054 | White |
| | +0.090 | −0.028 | +0.062 | Model |
| | | | $0.0642_{-0.0002}{}^{+0.0004}$ | Experimental |

neglected since they would be too close to the nucleus for the $r^2$ factor in the expression for $\mu_C$ to be important.

## DISCUSSION OF RESULTS

### Agreement between Experimental Results and Theoretical Calculations

The best predicted results are obtained by adding to the ion-pair solution the best predicted values for the nonslip part of the electronic contribution, $\mu_C$. Besides the value of $\mu_C$ obtained from the model, there are two published predicted values. One of these is by Foley[11] who gives a value for LiF (presumably Li⁷F) of 0.023 nuclear magneton. This would make the corresponding value for Li⁶F approximately 0.026 nuclear magneton. The second set of published values are those of White.[12] His values for the electronic sum appearing in the complete solution are $1.88\times10^{-44}$ g cm³ for Li⁶F and $1.87\times10^{-44}$ g cm³ for Li⁷F. This leads to the values 0.040 and 0.036 nuclear magneton for Li⁶F and Li⁷F, respectively. These values are all negative since they represent the rotation of negative charges. Table III compares the values described above with the experimental values.

The value of $H_n$ for Li⁶F has been measured.[18] A comparison between the results obtained from the semiclassical model for the electronic contribution and the experimental results is shown in Table IV.

The agreement between the model values and the experimental values indicates that the relative contributions of different parts of the charge distribution to $H_n$ and $\mu_C$ is fairly accurately represented in Fig. 11. The agreement should not, however, be thought of as verifying the charge distribution used since, with a suitable choice of $\alpha(r)$, any reasonable charge distribution which might be guessed would yield values for $H_n$ and $\mu_C$ in fair agreement with the measured values. The important point is that even for the new distribution the

[18] Kastner, Russell, and Trischka, J. Chem. Phys. 23, 1730 (1955).

TABLE IV. Comparison of calculated and experimental values for $\mu_C$ and $H_n$.

| | Experimental values | Calculated values |
|---|---|---|
| $\mu_C$ (nuclear magnetons)[a] | −0.031 | −0.033 |
| $H_n$ (gauss) | 9.01 | 8.34 |

[a] Obtained by subtracting ion-pair value from measured $\mu_J$ assuming the latter to be positive.

relative contributions of different parts of the charge distribution would be similar to that shown in Fig. 11.

## Conclusions

Rotational magnetic moments in alklai halide molecules can be described to first approximation by the rotation of two ions about their center of mass. This description indicates that the relative masses of the molecules can influence the sign of the moment.

A better approximation is achieved by taking into account the contribution from nonslipping electrons. This term is negative and arises because the electron motion about one ion is perturbed by the molecular rotation because the potential is distorted by the presence of the other ion. This is the same perturbation which gives rise to $J$ dependent magnetic fields at the nuclei. These magnetic fields which can be measured through the spin-rotation interaction do not determine the nonslip electronic contribution to the rotational magnetic moment since they arise largely from a different part of the charge distribution.

It is possible to construct a semiclassical model to describe the motion of the electronic charge cloud which gives good agreement with the values of both the spin-rotation interaction and the difference between the ion-pair value and the measured rotational magnetic moment of Li⁶F.

## ACKNOWLEDGMENTS

## APPENDIX. CLASSICAL CALCULATION OF ION-PAIR APPROXIMATION

Consider an alkali halide molecule made up of two singly charged ions of opposite sign. These ions will

TABLE V. Rotational magnetic moments of the alkali halides in nuclear magnetons per rotational quantum number as predicted by the ion-pair model.

| | F¹⁹ | Cl³⁵ | Cl³⁷ | Br⁷⁹,⁸¹ | I¹²⁷ |
|---|---|---|---|---|---|
| H¹ | +0.939 | +0.963 | +0.965 | +0.979 | +0.984 |
| H² | +0.444 | +0.468 | +0.469 | +0.484 | +0.488 |
| H³ | +0.279 | +0.303 | +0.304 | +0.319 | +0.324 |
| Li⁶ | +0.114 | +0.138 | +0.139 | +0.154 | +0.158 |
| Li⁷ | +0.090 | +0.114 | +0.116 | +0.130 | +0.135 |
| Na²³ | −0.009 | +0.015 | +0.016 | +0.031 | +0.036 |
| K³⁹ | −0.027 | −0.003 | −0.001 | +0.013 | +0.018 |
| K⁴¹ | −0.028 | −0.004 | −0.003 | +0.012 | +0.016 |
| Rb⁸⁵,⁸⁷ | −0.041 | −0.017 | −0.015 | −0.001 | +0.004 |
| Cs¹³³ | −0.045 | −0.021 | −0.020 | −0.005 | 0.000 |

have closed shells and they may be considered to have spherically symmetric charge distributions if the polarization of one ion by the electric field due to the other is neglected.

Since the electrons are in a spherically symmetric field the average angular momentum of the electronic charge distribution about the parent nucleus will be unaltered by the molecular rotation. This behavior of the electronic charge distribution is called complete slip. The angular momentum of the electrons about the nucleus with which they are associated is zero in the nonrotating case and, in this approximation, will remain zero when the molecule is rotating.

In this approximation each point in the electronic charge distribution moves in a circle of the same radius and at the same frequency as the parent nucleus (see Fig. 12). The rotational magnetic moment, $\mu_{AB}$, will arise from the net $+e$ charge of the positive ion and the $-e$ charge of the negative ion.

The general expression for a magnetic moment due to the motions of a collection of charges $i$ may be written

$$\mathbf{\mu} = \frac{1}{2c} \sum_i \left(\frac{e}{m}\right)_i (\mathbf{r}_i \times \mathbf{p}_i). \tag{1}$$

With these assumptions the rotational magnetic moment may be written

$$\mu_{AB} = \frac{1}{2c} \sum_i e_i r_i v_i = \frac{e\omega}{2c}(R_+^2 - R_-^2), \tag{2}$$

where $R_+$ and $R_-$ are the distances of the positive and negative ions from the center of mass of the molecule.
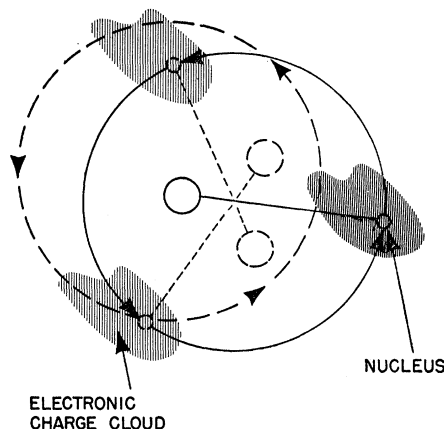


ELECTRONIC
CHARGE CLOUD

FIG. 12. A rotating ionic diatomic molecule showing that a particular part of the electronic charge cloud rotates in a circle of the same radius as the parent nucleus when complete slip is assumed.

Expression of this result in nuclear magnetons yields

$$\mu_{AB} = \frac{\omega m_p}{\hbar}(R_+^2 - R_-^2), \tag{3}$$

where $m_p$ is the proton mass.

The equation for the angular momentum is

$$J\hbar = M(R_+ + R_-)^2 \omega,$$

where

$$M = m_+ m_- / (m_+ + m_-).$$

The substitution of these values into (3) yields

$$\frac{\mu_{AB}}{J} = \frac{m_p}{M}\left(\frac{R_+ - R_-}{R_+ + R_-}\right). \tag{4}$$

Expression of the masses in atomic mass units, observing that $m_+ R_+ = m_- R_-$ gives the final result,

$$\frac{\mu_{AB}}{J} \cong \frac{1}{m_+} - \frac{1}{m_-} \tag{5}$$

nuclear magnetons per rotational state.

Table V shows the values of (5) for the alkali halides and the hydrogen halides. The latter are included because of their large ionic character.

Equation (5) neglects the interaction between the electrons and the molecular frame due to the deviation of the electric fields from spherical symmetry in the presence of the other ion. This consideration gives rise to an additional contribution, $\mu_C$, called the nonslip part, which is included in the complete solution.